Axial Dispersion in Taylor-Couette Flow

Christine M. V. Moore and Charles L. Cooney
Dept. of Chemical Engineering and Biotechnology Process Engineering Center, Massachusetts Institute of Technology, Cambridge, MA 02139

The vortex flow induced by the rotating core of a concentric cylindrical annulus is the basis of numerous chemical and biomedical applications. The torroidal vortices formed with or without the presence of axial flow occur when the rotation rate of the inner cylinder exceeds a critical value. G. I. Taylor (1923) first determined the critical rotation speed for vortex formation without axial flow. The following 70 years of research have yielded a vast amount of information on the hydrodynamics, transport properties and applications of Taylor-Couette vortex columns. Some practical applications of vortex flow presented over the years include: catalytic chemical reactors (Cohen and Moalem Maron, 1983), filtration devices (Holeschovsky and Cooney, 1991), blood plasmaphoresis devices (Beaudoin and Jaffrin, 1989), plant cell bioreactors (Janes et al., 1987), ion exchangers (Olin et al., 1954), and liquid-liquid extractors (Davis and Weber, 1960).

Design, scaleup and optimization calculations for vortex flow reactors require a complete understanding of the transport properties of Taylor-Couette flow. While some transport properties, such as mass and heat transfer to the cylinder walls, have been well described in the literature, backmixing or dispersion in vortex flow systems has received considerably less attention. Dispersion is an important factor in reactor design as the amount of mixing within the vortices greatly influences the productivity of a reactive system. Mixing in Taylor-Couette flows occurs in circumferential, radial and axial directions. Kataoka and coworkers (1975) showed that the rate of circumferential and radial mixing is fast compared to axial mixing. Consequently, axial dispersion is the dominant parameter in designing reactive vortex flow systems. To completely describe axial dispersion in the vortex flow systems, it is necessary to understand the effects of operational parameters and design parameters. Previous studies of axial mixing in vortex flow have focused on operation at extreme high or low rotation rates, typically without axial flow and without regard to the effect of reactor geometry. The objective of this work was to experimentally study and mathematically describe axial dispersion in vortex flow for a wide range of operational parameters (rotation rate, axial flow rate) and design parameters (reactor geometry).

A common goal in reactor design is to approach plug flow by maximizing mixing in the cross-sectional (radial and circumferential) directions while minimizing mixing in the axial direction. Taylor-Couette vortex flow fits the description of plug-flow behavior at low rotation rates and low axial flow rates (Kataoka et al., 1975; Pudjiono et al., 1992). This flow behavior corresponds to rotation rates of the inner cylinder just above the critical value when the vortices exist in laminar, closed streamlines. As the rotation rate increases, the vortices begin to overlap as visualized by the commencement of spiral vortex flow in narrow gap ($b/r_i < 0.4$) vessels. The first signs of turbulence appear at rotation rates approximately 10 times the critical rate (DiPrima and Swinney, 1981). Nevertheless, the flow retains its characteristic vortex structure. Smith and Townsend (1982) report the persistence of vortex structure up to 500 times the critical rotation rate.

Other researchers have examined axial mass transport in turbulent vortex flow. Tam and Swinney (1987) examined axial dispersion in Taylor-Couette flow without axial flow for rotational (azimuthal) Reynolds numbers (Re_θ) between 100 to 1,000 times the critical value and the gap ratio (b/r_i) from 0.14 to 1.0. The measured axial dispersion coefficients were found to vary as the power law $D^* \sim (Re_\theta)^{\beta}$, with the exponent β dependent on reactor geometry. Related torque studies (Lathrop et al., 1992) imply that the exponent β may not be a fixed value but rather increase with increasing Re_θ. Enokida and coworkers (1989) also measured axial dispersion coefficients in turbulent vortex flow for the gap ratios of 0.32 and 0.69 with rotational Reynolds numbers ranging from 30 to 500 times the critical value. They found a slightly different power law, $D^* \sim (r_{avg}\ \omega^2)^{\beta}$ for dispersion in vortex flow without axial flow. The increase in the dispersion coefficient upon the introduction of axial flow was roughly proportional to the azimuthal velocity component, $Re_\theta u$.

The study described here examines axial dispersion in a vortex flow reactor operating at 4 to 200 times the critical rotation rate with gap ratios ranging from 0.04 to 0.38 and with axial Reynolds numbers ranging from 0.5 to 30. The correlation derived from this experimental study describes axial dispersion as a function of the operational and geometric parameters. Dispersion coefficients are found to range from 0.01 to 10 cm^2/s, indicating that vortex flow system operation varies from well-stirred flow to near-plug flow.

Experimental Method

The vessel design is based on the Membrex (Fairfield, NJ) Benchmark vortex flow filtration system. The vessel consists of two concentric cylinders forming an annulus. The outer

polysulfone cylinder is stationary, and the inner polypropylene cylinder is rotated with a variable speed motor. Rotation rates from 0 to 2,000 rpm are obtained with a Membrex motor connected to a separate controller (Electro-Craft E652-M). The motor and controller of the commercial Membrex filtration unit are used to achieve rotation rates between 2,000 and 4,000 rpm. The cylinder rotation rate, determined with a tachometer, is accurate to at least 1%.

Outer cylinders of varied diameters were obtained by machining the commercially available Membrex cylinders. To eliminate stagnant zones within the vessel, the outer (retentate) port was repositioned at the top of the cylinder opposite the inlet port and the filtrate ports were blocked off. In addition, a metal pin was inserted in the bottom of the outer cylinder to provide a truer rotation of the inner cylinder. Inner cylinders of varied diameters were machined from solid polypropylene. The dimensions of the 17 cm long cylinders used in the experiments are shown in Table 1. The cylinders provided gap ratios ranging from 0.045 to 0.38 and aspect ratios from 22 to 370. An additional set of longer cylinders with length of 25.2 cm, inner cylinder diameter of 5.35 cm and an outer cylinder diameter 6.23 cm was also made, providing a gap ratio of 0.16 and an aspect ratio of 57. Table 1 also includes critical rotational Reynolds numbers for the cylinders; these numbers are calculated using the stability criteria for Taylor-Couette flow with no axial flow (Taylor, 1923).

Axial dispersion is determined from residence time distribution studies. The working fluid in all experiments was deionized water or water and glycerol. Fluid enters through a port at the base of the annulus and exits from the top port, opposite the inlet. At the initiation of each run, a tracer of either blue dextran (5×10^{-5} M) or sodium benzoate (0.14 M) was injected into the annulus via a 4-way chromatography valve. The outlet concentration of the tracer was measured with a flow-through UV spectrophotometer at a wavelength of 280 nm. All tubing, including the sample loop, had an inner diameter of 1.5 mm. Both the injection sample and hold-up volume (tubing volume before and after annulus) were held to a minimum, less than 1% of the annulus volume. The flow rate was varied to provide axial Reynolds numbers between 0.5 and 30. All experiments were performed at room temperature (298 ± 3 K); at high rotation rates a water bath was used to maintain temperature.

Mathematical Formulation

Transport of a species of concentration $C(r,t)$ in an incompressible fluid is given by:

$$\frac{\partial C(r,t)}{\partial t} + v(r,t)\cdot\nabla C(r,t) = D_{mol}\nabla^2 C(r,t) \qquad (1)$$

where $v(r,t)$ is the fluid velocity and D_{mol} is the molecular diffusion coefficient. By virtue of the spatial periodicity of Taylor-Couette flow, Eq. 1 can be simplified to a one-dimensional (1-D) dispersion-convection equation provided two criteria are met (Tam and Swinney, 1987):

(1) The length of the test section is large compared to the vortices.

(2) The tracer is well mixed within the vortex in the radial and azimuthal directions on a time scale that is short compared to transport in the axial direction.

As transport in the axial direction occurs both by convection and dispersion, both of these time scales must be greater than the time scale for mixing in an individual vortex. The corresponding 1-D transport equation is:

$$\frac{\partial \bar{C}(z,t)}{\partial t} + U\cdot\frac{\partial \bar{C}(z,t)}{\partial z} = D^*\frac{\partial^2 \bar{C}(z,t)}{\partial z^2} \qquad (2)$$

where $\bar{C}(z,t)$ is the normalized, vortex-averaged concentration of tracer at axial position z, U is the average velocity of the carrier fluid, and D^* is the effective diffusivity or dispersion coefficient. The boundary conditions:

$$\bar{C}(z,0) = \delta(z)\delta(t) \qquad (2a)$$

$$-D^*\frac{\partial \bar{C}(0,t)}{\partial z} + U\bar{C}(0,t) = 0 \qquad (2b)$$

$$-D^*\frac{\partial \bar{C}(L,t)}{\partial z} = 0 \qquad (2c)$$

assume an instantaneous pulse of tracer at $(z,t)=(0,0)$, and no back flow across the inlet and outlet ports or in the short sections of tubing before or after the vessel. The concentration profile at the vessel outlet (Yagi and Miyauchi, 1953) is:

$$\bar{C} = \sum_{i=1}^{\infty}\frac{\lambda_i Pe(Pe\sin\lambda_i + 2\lambda_i\cos\lambda_i)}{\left(\frac{Pe}{2}\right)^2 + Pe + \lambda_i}\exp\left[\frac{Pe}{2} - \left(\frac{Pe}{4} + \frac{\lambda_i^2}{Pe}\right)\tilde{t}\right] \qquad (3)$$

$$\cot\lambda_i = (\lambda_i/Pe - Pe/4\lambda_i)$$

where $Pe = uL/D^*$ is the Peclet number and $\bar{C}$ and $\tilde{t}$ are dimensionless concentration and time, respectively.

The macrotransport parameter D^* in Eq. 2 has been mathematically related to physical parameters in spatially periodic systems such as Taylor-Couette flow for cases: without reaction (Brenner, 1980), with reaction on the walls (Shapiro and Brenner, 1988), and with reaction on particles suspended in the annulus (Iosilevskii et al., 1993). However, solving these

Table 1. Dimensions of Inner and Outer Cylinders

	Inner Cylinder Diameter											
	4.45 cm			4.21 cm			3.81 cm			4.69 cm		
Outer Cylinder	b/r_i	L/b	Critical Re_θ	b/r_i	L/b	Critical Re_θ	b/r_i	L/b	Critical Re_θ	b/r_i	L/b	Critical Re_θ
4.90 cm	0.101	75	137	0.164	49	112	0.286	31	90.9	0.045	161	199
5.19 cm	0.166	46	111	0.233	35	97.5	0.362	25	84.6			
5.76 cm	0.294	26	90	0.368	22	84.3						

equations involves complicated numerical calculations requiring detailed knowledge of the velocity profile. An alternative approach used here is to describe dispersion through a semi-empirical analysis using experimental data.

Data Analysis

Analysis of residence time distribution (RTD) curves employed the coefficient of quartile variation (CoQV), a statistical parameter, defined as (Beyer, 1981):

$$\text{CoQV} = 100\frac{t_{3/4} - t_{1/4}}{t_{3/4} + t_{1/4}} \tag{4}$$

where $t_{1/4}$ and $t_{3/4}$ are, respectively, the times for one-quarter and three-quarters of the RTD curve to emerge. During data analysis, the CoQV of the experimental curve is determined. Then, a dispersion coefficient is guessed and Eq. 3 is numerically integrated to determine the CoQV. The dispersion coefficient is then iteratively adjusted until the calculated and experimental CoQV values matched. Following calculation of CoQV and D^*, the experimental data are plotted with the curve reconstructed from Eq. 3 to check for agreement with the 1-D transport model. Peclet numbers calculated from duplicate runs and analyzed by the CoQV method were reproducible to within 10% for $Pe > 0.05$. For very high dispersion with $Pe < 0.05$, the Peclet number cannot be accurately determined due to numerical limitations.

In the operational ranges studied, two areas of violation of the 1-D assumption were observed. At low rotation rates, especially in vessels with a large annular gap, periodic spikes occurred on the RTD curves indicating signs of incomplete azimuthal mixing. Although the data still fit fairly well to the dispersion model Eq. 3, they were not used in further analysis. The second violation of the 1-D assumption occurs at high axial flow rate where the RTD curves showed an early, sharp rise and a long decay not characteristic of the dispersion model Eq. 3. This case corresponds to a violation of the "long-term limit" where the tracer does not have sufficient time to sample both the fast and slow moving velocity streamlines. Because the time scale for convection varies as L/u, this problem can be circumvented by either lowering the axial velocity or increasing the length of the annulus. These trends were observed experimentally.

Results

The calculated dispersion coefficients, ranging from 0.01 to 10 cm^2/s, are several orders of magnitude greater than the molecular diffusivity of the tracer thus indicating the importance of convection in the reactor. Several series of experiments were undertaken to establish the dependency of dispersion on the geometric and operational parameters.

Effect of tracer diffusion coefficient

Tracers of blue dextran ($D_{mol} = 8\times10^{-8}$ cm^2/s) and sodium benzoate ($D_{mol} = 8\times10^{-6}$ cm^2/s) were used to determine if diffusion plays a role in transport. The experiments were conducted using a large gap ratio ($b/r_i = 0.36$) at low rotation rates ($Re_\theta = 150$–$1{,}000$) and low axial flow rate of $Re_z = 0.6$.

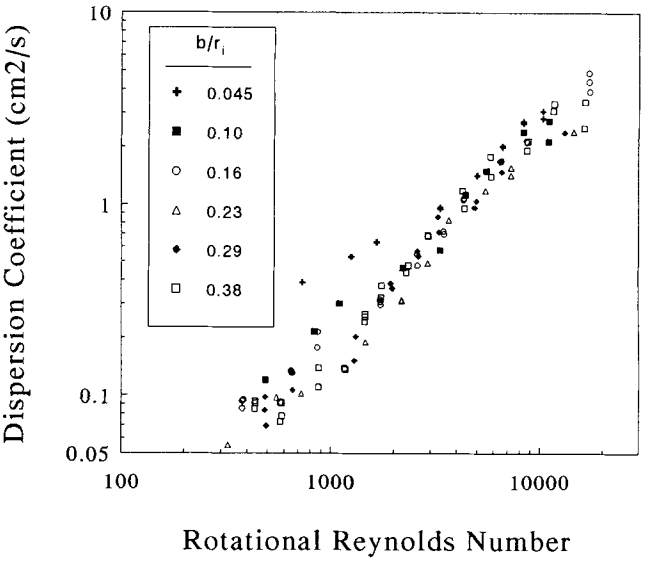

Figure 1. Effect of gap ratio on axial dispersion.

Although the diffusion coefficients varied by a factor of 100, there was no difference in the axial dispersion, indicating that diffusion has no effect on axial dispersion throughout the experimental regions studied.

Effect of gap ratio

To determine the effect of the gap ratio on dispersion, nine sets of experiments were conducted at a constant axial Reynolds number, $Re_z = 5.0$. Each set used a different combination of inner and outer cylinders and spanned a wide range of angular Reynolds numbers, Re_θ. The results, shown in Figure 1, indicate that dispersion is a strong function of Re_θ and has little dependence on the gap ratio. Regression of the data provides $D^* \sim (b/r_i)^{-0.28}$.

End effects

Dispersion experiments were conducted in a long reactor to determine if end effects have a significant influence on the measured dispersion coefficients. The cylinder used was approximately 50% longer than those in the previous experiments. Figure 2 shows no discrepancies between dispersion coefficients obtained from long and short cylinders with the same gap ratios, thus indicating that end effects are negligible in the region studied.

Effect of operational parameters

To determine the effect of Re_θ and Re_z on dispersion, sets of dispersion experiments were performed with Re_z ranging from 0.5 to 30. The data reveal that dispersion is primarily dependent upon Re_θ with little dependence on Re_z. Regression of the data at each of the axial Reynolds numbers shown in Table 2 provides Re_θ exponents ranging from 0.9 to 1.1. When the data are regressed together, the relationship:

$$D^* \propto (b/r_i)^{-0.28} Re_\theta^{1.05} Re_z^{0.17} \tag{5}$$

fits the data with an average error of 17%. The regression fit is plotted against the data in Figure 3. The equation in di-

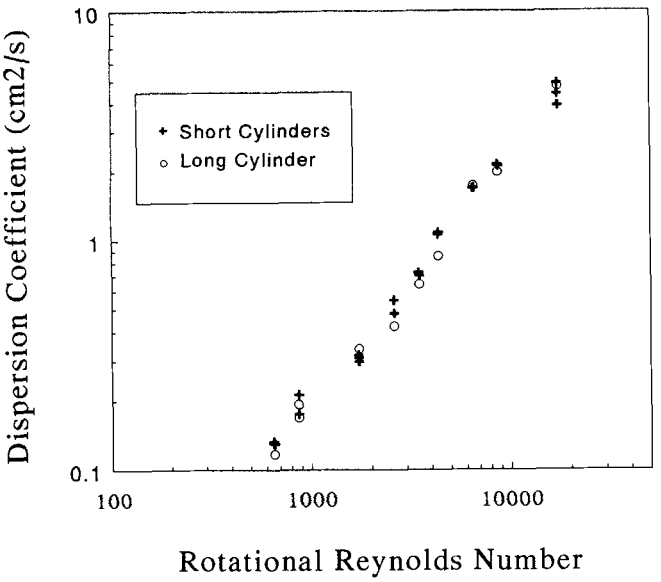

Figure 2. Effect of cylinder length on axial dispersion.

Short cylinder is 16.9 cm long long with gap ratio = 0.164; long cylinder is 25.2 cm long with gap ratio of 0.164.

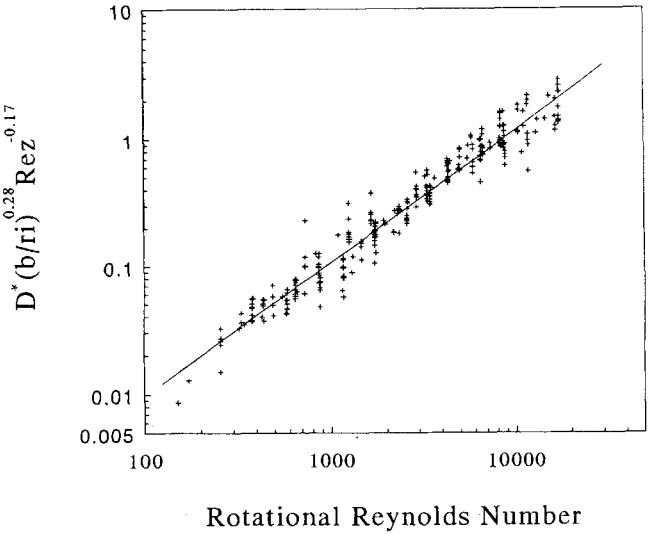

Figure 3. Regression fit of all dispersion experiments.

mensionless form can be written as:

$$Pe^{-1} = 7.2\times10^{-3}(b/r_i)^{-0.28} Re_\theta^{1.05} Re_z^{-0.83}(2b/L) \quad (6)$$

Effect of viscosity

While viscosity appears in the Reynolds numbers in Eq. 6, it was not used as a variable in developing the correlation. Therefore, the effect of viscosity provides an opportunity for independent verification of the correlation. Figure 4 shows the experimental values and correlation predictions for RTD studies using $Re_z = 5$ and glycerol-water solutions of 25 and 45% with kinematic viscosities of 0.018 and 0.037 cm^2/s, respectively. Good agreement is found in support of the correlation.

Discussion

The dispersion correlation described by Eq. 6 provides a basis for design and scale-up of vortex flow systems over a wide operating range. The operational range is known to cover several flow regimes of Taylor-Couette flow including laminar, wavy and turbulent vortices.

Table 2. Regression Parameters from Dispersion Experiments

Re_z	Coefficient	Exponent
0.50	3.9×10^{-5}	1.11 ± 0.06
1.1	6.9×10^{-5}	1.05 ± 0.04
2.5	9.7×10^{-5}	1.05 ± 0.03
8.0	1.3×10^{-4}	1.02 ± 0.03
15	1.6×10^{-4}	1.00 ± 0.03
30	3.0×10^{-4}	0.92 ± 0.03

Although the vortex structures in the three flow regimes are very different, no sudden change or discontinuity in dispersion was evident to signify a change in flow pattern or the onset of turbulence. The lack of a sharp transition is reflective of the gradual change in hydrodynamics as the vortices become increasingly turbulent.

Perhaps the most surprising result of these experiments is the independence of dispersion on the diffusion coefficient. The experiments with tracers of different diffusivities were performed at low axial Reynolds number of 0.6 and with a wide gap geometry of $b/r_i \approx 0.4$ where laminar vortices are known to exist (Gu and Fahidy, 1985). If the vortex cells are truly laminar and nonoverlapping, transport between cells can only occur by diffusion across the separatrix between the vortices. Theory of dispersion in spatially periodic systems (Rosenbluth et al., 1987) predicts that in this case D^* should vary as $(D_{mol}\, u_v b)^{1/2}$ where u_v is the characteristic vortex velocity. Therefore, we would expect a 10-fold increase in dispersion due to the 100-fold increase in the diffusion coef-

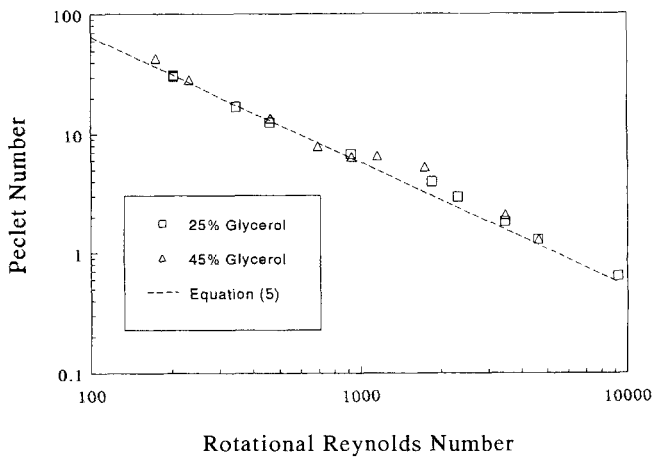

Figure 4. Effect of viscosity on axial dispersion.

ficient. Instead we find dispersion to be independent of the diffusion coefficient. In addition, if we estimate the value of $(D_{mol}\, u_v b)^{1/2}$ by using the maximum velocity in the vortex of $u_v = \omega r_i$, we find the theoretical value of the dispersion coefficient to be at least one order of magnitude lower than the experimentally measured D^*. These findings suggest a convective interchange across the vortex boundaries possibly caused by the small applied axial flow.

It is difficult to compare the work in the present study with those of other authors as most used a different range of rotational Reynolds numbers and no axial flow. The 1.05 Re_θ exponent in Eq. 6 is slightly higher than the 0.69 to 0.86 exponent found by Tam and Swinney (1987) or Enokida et al. (1989) in their studies on dispersion in Taylor-Couette flow without axial flow. Although the form of the correlation is different, the magnitudes of the measured dispersion coefficients are comparable. The correlation used by Enokida and coworkers to fit axial dispersion data in Taylor-Couette flow with axial flow is different from that in the present work. The axial Reynolds numbers used in the experiments, ranging from 60 to 250, are much higher than in this study. The data from their experiments are suspect as it is likely that the long-term limit assumed in the 1-D model was violated because of the high axial flow rates.

Over a 100-fold difference is obtained between dispersion coefficients at the highest and lowest rotation rates examined. For the current vessel, this corresponds to near plug-flow performance at the lowest rotation rates and stirred tank (CSTR) performance at the highest rotation rates. Unlike other solid-liquid reactors (that is, traditional fluidized-bed, tubular reactors), dispersion in the Taylor-Couette system is primarily independent of flow rate. This is a useful feature for reactor control as the extent of reaction can be adjusted independently of the flow rate. Of course, an additional consideration in performance of a reactive vortex flow system is mass transfer to the active surface. This problem is being addressed in separate experimental work and together with the results presented here provide a basis for reactor modeling. As both mass transfer and dispersion increase with an increased rotation rate, an optimization problem is expected to result.

Acknowledgments

The authors wish to acknowledge support from the National Science Foundation to the Biotechnology Processing Engineering Center under the Engineering Research Center Initiative (Cooperative Agreement ECD-88-03014), and from the National Institutes of Health under the Interdepartmental Biotechnology Training grant (#5 T32 GM08334) and under Public Service grant 1R01 GM25810-01. The authors also wish to thank Membrex, Inc. for equipment, and Rob Davis (U. Colorado-Boulder) for discussions on fitting RTD curves.

Notation

$b = r_o - r_i$ = gap width
$\bar{c}$ = vortex averaged concentration
L = reactor length
r_i, r_o = inner, outer radius
$Re_\theta = \omega r_i b/\upsilon$ = rotational Reynolds number
$Re_z = 2ub/\upsilon$ = axial Reynolds number
u = average axial velocity
z = axial coordinate

Greek letters

ν = kinematic viscosity
ω = rotation rate of inner cylinder

Literature Cited

Beaudoin, G., and M. Y. Jaffrin, "Plasma Filtration in Couette Flow Membrane Devices," *Artif. Organs*, **13**(1), 43 (1989).
Beyer, W. H., *CRC Standard Mathematical Tables*, CRC Press, Boca Raton, FL (1981).
Brenner, H., "Dispersion Resulting from Flow Through Spatially Periodic Porous Media," *Phil. Trans. R. Soc. Lond.*, **A 297**, 81 (1980).
Cohen, S., and D. Moalem Maron, "Experimental and Theoretical Study of a Rotating Annular Flow Reactor," *Chem. Eng. J.*, **27**, 87 (1983).
Davis, M. W., and E. J. Weber, "Liquid-Liquid Extraction Between Rotating Concentric Cylinders," *Ind. Eng. Chem.*, **52**(11), 929 (1960).
DiPrima, R. C., and H. L. Swinney, "Instabilities and Transition in Flow Between Concentric Rotating Cylinders," *Hydrodynamic Instabilities and the Transition to Turbulence*, Springer-Verlag, New York, pp. 139–180 (1981).
Enokida, Y., K. Nakata, and A. Suzuki, "Axial Turbulent Diffusion in Fluid Between Rotating Coaxial Cylinders," *AIChE J.*, **35**(7), 1211 (1989).
Gu, Z. H., and T. Z. Fahidy, "Visualization of Flow Patterns in Axial Flow Between Horizontal Coaxial Rotating Cylinders," *Can. J. Chem. Eng.*, **63**, 14 (1985).
Holeschovsky, U. B., and C. L. Cooney, "Quantitative Description of Ultrafiltration in a Rotating Filtration Device," *AIChE J.*, **37**(8), 1219 (1991).
Iosilevskii, G., H. Brenner, C. M. V. Moore, and C. L. Cooney, "Mass Transport and Chemical Reaction in Taylor-Vortex Flows with Entrained Catalytic Particles: Application to a Novel Class of Immobilized Enzyme Biochemical Reactors," *Phil. Trans. R. Soc.*, **345**, 259 (1993).
Janes, D. A., N. H. Thomas, and J. A. Callow, "Demonstration of a Bubble-Free Annular-Vortex Membrane Bioreactor for Batch Culture of Red Beet Cells," *Biotech. Tech.*, **1**(4), 257 (1987).
Kataoka, K., H. Doi, and T. Hongo, "Ideal Plug-Flow Properties of Taylor Vortex Flow," *J. Chem. Eng. Japan*, **8**(6), 472 (1975).
Lathrop, D. P., J. Fineberg, and H. L. Swinney, "Turbulent Flow between Concentric Rotating Cylinders at Large Reynolds Number," *Phys. Rev. Lett.*, **68**(10), 1515 (1992).
Olin, J., W. W. Koenig, A. L. Babb, and J. L. McCarthy, "Continuous Countercurrent Ion Exchange: I. Resin Particle Settling Rates in Spiner Columns," *AIChE Symp. Ser.*, **50**(14), 103 (1954).
Pudjiono, P. I., N. S. Tavare, J. Garside, and K. D. P. Nigam, "Residence Time Distribution from a Continuous Couette Flow Device," *Chem. Eng. J.*, **48**, 101 (1992).
Rosenbluth, M. N., H. L. Berk, I. Doxas, and W. Horton, "Effective Diffusion in Laminar Convective Flows," *Phys. Fluids*, **30**(9), 2636 (1987).
Shapiro, M., and H. Brenner, "Dispersion of a Chemically Reactive Solute in a Spatially Periodic Model of a Porous Medium," *Chem. Eng. Sci.*, **43**(3), 551 (1988).
Smith, G. P., and A. A. Townsend, "Turbulent Couette Flow Between Concentric Cylinders at Large Taylor Number," *J. Fluid Mech.*, **123**, 187 (1982).
Tam, W. Y., and H. L. Swinney, "Mass Transport in Turbulent Couette-Taylor Flow," *Phys. Rev. A*, **36**, 1374 (1987).
Taylor, G. I., "Stability of a Viscous Liquid Contained between Two Rotating Cylinders," *Phil. Trans. Roy. Soc.*, **A 223**, 289 (1923).
Yagi, S., and T. Miyauchi, "On the Residence Time Curves of the Continuous Reactors," *Kagaku Kogaku*, **17**, 382 (1953).

Manuscript received Nov. 17, 1993, and revision received Apr. 22, 1994.